Am J Transl Res 2021;13(6):6431-6438
www.ajtr.org /ISSN:1943-8141/AJTR0131076

Original Article

A comparative analysis of CT and MRI in differentiating pancreatic cancer from mass pancreatitis

Song Jiang, Yongmei Li

Department of Radiology, The First Affiliated Hospital of Chongqing Medical University, Chongqing 400016, China

Received January 30, 2021; Accepted March 17, 2021; Epub June 15, 2021; Published June 30, 2021

Abstract: Aim: This paper aims to explore the practical value of CT signs combined with magnetic resonance imaging with diffusion-weighted imaging (MRI-DWI) and magnetic resonance cholangiopancreatography (MRCP) in the differential diagnosis of pancreatic carcinoma and mass-forming pancreatitis. Methods: We carried out a retrospective analysis of the imaging data of 61 patients with pancreatic mass lesions who were diagnosed based on postoperative pathology in our hospital from May 2013 to May 2020 and analyzed the image diagnostic value of the combination of 128-slice CT and 1.5T MRI-DWI. Results: There were no significant differences in the pancreatic duct dilatation, the bile duct dilatation, or the peripancreatic and retroperitoneal lymph node enlargement between the patients with pancreatic carcinoma and the patients with mass-forming pancreatitis *(P > 0.05)*. Both the incidences of lobulation signs and peripancreatic vascular invasion in the patients with pancreatic carcinoma were higher than they were in the patients with mass-forming pancreatitis, and the mass calcification, pseudocyst, and pancreatic duct stone rates, the net enhanced CT values in the arterial and pancreatic parenchyma phases, and the ADC values in pancreatic carcinoma patients were lower than they were in the patients with mass-forming pancreatitis (*P < 0.05*). The pancreatic duct stone and right prerenal fascial thickening rates in the patients with pancreatic carcinoma were lower than they were in the patients with mass-forming pancreatitis (P < 0.05). Conclusion: CT signs combined with the MRI-DWI technique and MRCP can improve clinical pancreatic cancer diagnostic sensitivity.

Keywords: CT signs, magnetic resonance, magnetic resonance diffusion imaging, pancreatic cancer, mass-forming pancreatitis

Introduction

Mass-forming pancreatitis is a special type of chronic pancreatitis, and its main changes involve varying degrees of fibrosis accompanied by glandular atrophy. The lesions are manifested by enlargement and accompanied by mass formation. The characteristics are similar to the imaging findings of pancreatic cancer, so the two diseases are often misdiagnosed. As their treatment is totally different, it is of great clinical significance to have accurate preoperative diagnoses for the patients [1, 2]. Although surgical biopsy and needle aspiration biopsy are the gold standards for the differential diagnosis of pancreatic masses, these procedures increase the patients' risks of infection and bleeding [3]. Therefore, non-invasive examinations such as endoscopic ultrasound, CT, and MRI are still the first choice for patients. Recently, MRI-DWI has gradually showed its diagnostic efficiency because of its dispersion and dynamic distribution of water molecules. The diagnostic value of magnetic resonance cholangiopancreatography (MRCP) for the bile duct has also gradually been confirmed. MRCP, a non-invasive operation that is relatively safe, non-invasive, and non-radioactive in its clinical application, is easily accepted by patients [4-6].

Previous studies initially showed the value of CT signs in the clinical differential diagnosis of mass-forming pancreatitis and pancreatic cancer; however, a single imaging examination cannot obtain sufficient sensitivity [7]. Therefore, the purpose of this study is to carry out a comparative analysis of CT signs combined with MRI-DWI and MRCP in the differential diagnosis of pancreatic carcinoma and mass-forming pancreatitis and to provide theoretical support for the early clinical diagnosis of pancreatic masses.

The baseline data and methods

The baseline data

All of the 61 patients with pancreatic mass lesions diagnosed through operations and pathology in our hospital from May 2013 to May 2020 were recruited for this study, including those with pancreatic carcinoma (n = 31) and mass-forming pancreatitis (n = 30). Inclusion criteria: (1) The pancreatic carcinoma and mass-forming pancreatitis lesions are located in the head of the pancreas and confirmed by pathology. (2) Patients with non-ductal epithelial pancreatic neuroendocrine neoplasms. Exclusion criteria: (1) Patients comorbid with other tumors. (2) Patients with mental disorders. (3) Patients with infectious diseases. (4) Patients who were contraindicated for MRI and CT. (5) Patients with missing data. The study was approved by the institutional ethics committee of The First Affiliated Hospital of Chongqing Medical University and was conducted in accordance with the Declaration of Helsinki. Written informed consent was obtained from all the patients before their participation in the study.

Methods

CT scans: The patients assumed a supine position and were scanned with a 28-slice spiral CT (Somatom Definition Flash Spiral CT, Siemens), from the diaphragmatic dome to the inferior margin of the pubic symphysis, the scanning parameters were as follows: voltage of 120 kV, current of 200 mA, slice thickness of 5 mm, layer spacing of 5 mm, and a pitch of 0.8. At the same time, we used the scanned raw data to perform multiplanar reformatting in the coronal, sagittal, and arbitrary positions. CT enhanced scan: 300 mg/mL of iohexol was injected through the elbow vein using a high-pressure syringe, the amounts were 60-100 mL, and the rate was controlled to 3 mL. The patients were scanned in the pancreatic parenchymal stage (delay time 35 s), the venous phase (delay time 60 s) and the delay period (delay time 120 s) with the same range as the plain scan.

MRI-DWI scan: A 1.5 T superconducting magnetic resonance scanner (GE Healthcare, Wisconsin, USA) with an abdominal phased-array surface coil was used for the scan. The supine position was taken for the routine cross-sectional scans. The patients were examined using T1WI, T2WI and DWI, and the scanning parameters were as follows: T1WI uses the fast gradient echo fat compression sequence, TR = 185 ms, TE = 3.1 ms, layer thickness = 6 mm, layer distance = 2 mm. Axial positive and negative phase T1 non-pressing sequences with the scan parameters were as follows: single breath-holding TR = 200 ms, TE = 2.2 ms (opposed), 4.8 ms (in), slice thickness = 6 mm, layer spacing = 1 mm. T2WI uses the breath-triggered fat suppression spin echo sequence, and the scan parameters were as follows: TR = 6000-7500 ms, TR = 6000-7500 ms, 86.7 ms, slice thickness = 6 mm, layer spacing = 2 mm. The single-shot spin echo echo-planar image (SS-SE-EPI) sequence was used for DWI, and the respiratory gating technique parameters were as follows: TR = 6666.7 ms, TE = 69.0 ms, FOV = 42 cm, matrix = 228X224, layer thickness = 6 mm, layer spacing = 2 mm, NEX = 2, using b value = 0 and 600 s/mm^2.

Image post-processing and analysis: The scanned data were transmitted to the ADW4.4 workstation, where a circular region of interest (ROI) is used to measure the ADC value (mean ± standard deviation). If the reference b value is too large or too small, it will affect the strength, so this study chose b = 600 s/mm^2. In order to locate the lesions accurately on the ADC map, T2WI was used as a reference. Pancreatic carcinoma and mass-forming pancreatitis ROIs should be placed at the largest central level of the lesion to avoid including the normal pancreatic tissue. The size of the ROIs should be adjusted according to each lesion, and attention should be paid to avoid all blood vessels, necrosis, bleeding, cystic degeneration, and calcification areas.

Evaluation indicators

The images were diagnosed and analyzed by two senior deputy chief physicians. The observation indicators were as follows: CT mainly includes mass lobulation, calcification, necrosis, cysts, pseudocysts, pancreatic duct stones, enhanced net CT values, whether the peripheral blood vessels are invaded, and whether the surrounding tissues are changed. The main indicators of MRI-DWI and MRCP were as follows: the ADC values, the degree of dilatation of the main pancreatic duct and the common bile

Table 1. Comparison of the baseline data between the two groups ($\bar{x} \pm s$)

Groups	n	Gender (male/female)	Average age (years)	Biliary disease (%)	Pancreatic disease (%)
pancreatic cancer	30	21/10	66.03±12.20	5 (16.67)	3 (10.00)
Massive pancreatitis	31	28/2	55.58±12.75	25 (80.65)	22 (70.97)
X^2/t		6.319	3.269	27.550	24.754
P		0.012	0.002	0.001	0.001

duct, the invasion of the peripheral blood vessels and the concomitant changes in the surrounding tissue. The two types of diseases were compared and analyzed.

Statistical processing: SPSS 22.0 statistical software was used for the analysis, the measurement data were tested to be in accordance with a normal distribution, and they were expressed as the mean ± standard deviation ($\bar{x} \pm SD$). Independent sample t-tests were used for the comparisons between the two groups, and the number of cases in the enumeration data was expressed as a percentage [n (%)]. The comparisons were done using chi-square tests, and a difference was statistically significant when $P < 0.05$.

Results

Comparison of the baseline data between the two groups

The results of this study showed that males have a high incidence of pancreatic diseases, and the incidence of pancreatic carcinoma in females is higher than it is in patients with mass-forming pancreatitis (X^2/t = 6.319, P = 0.012). The pancreatic carcinoma onset age is higher than it is in patients with massive pancreatitis, but the incidence of complications such as biliary and pancreatic lesions are lower than they are in patients with mass-forming pancreatitis (X^2/t = 3.269, 27.550, 24.754, all $P < 0.05$) (**Table 1**).

Comparison of the imaging features among the patients in the two groups

The mass diameter in the mass-forming pancreatitis patients was (3.56±2.05) cm, and the mass diameter in the pancreatic carcinoma patients was (3.04±1.46) cm, so there was no difference between the two groups of patients (X^2/t = 1.138, P = 0.260). The number of signs of lobulation that occurred in the mass-forming pancreatitis patients was 4 (12.90%), and in the pancreatic carcinoma patients it was 25 (83.33%), so there was a significant difference between the two groups of patients (X^2/t = 30.324, P = 0.001). The incidences of mass calcification in the mass-forming pancreatitis patients and the pancreatic carcinoma patients respectively were 58.06% (18/31) and 3% (10/30), and the difference was statistically significant (X^2/t = 16.120, P = 0.014). The incidences of pancreatic duct dilatation in the two groups were 45.38% (15/31) and 16.7% (5/30), respectively, with a significant difference (X^2/t = 16.120, P = 0.014). The incidences of bile duct dilatation in the two groups were 70.97% (22/31) and 53.33% (16/30), respectively, with no significant difference (X^2/t = 2.018, P = 0.155). The enhancement degree in the mass-forming pancreatitis patients in the arterial and portal phases was higher than it was in the pancreatic carcinoma patients, and the difference in the net enhancement CT values was statistically significant (X^2/t = 5.172, 2.984, P = 0.001, 0.004). The incidence of peripancreatic vascular invasion in the mass-forming pancreatitis patients was 70.97% (22/31), and in the pancreatic carcinoma patients it was 80%, and there was no significant difference (X^2/t = 0.531, P = 0.562). The incidences of enlarged peripancreatic and retroperitoneal lymph nodes in the two groups were 45.16% (14/31) and 70% (21/30), with no significant difference (X^2/t = 2.769, P = 0.096). The incidences of high signals on DWI in the two groups were 9.68% (3/31) and 53.33% (16/30), with a significant difference (X^2/t = 11.589, P = 0.001). The results of this study showed that there were no significant differences in terms of the mass diameters, the pancreatic duct dilatation, the bile duct dilatation, or the peripancreatic and retroperitoneal lymph node enlargement rates in the pancreatic carcinoma and mass-forming pancreatitis patients (P > 0.05). The

Table 2. Comparison of the imaging features between the patients with pancreatic carcinoma and mass-forming pancreatitis ($\bar{x} \pm s$)

Imaging features	Mass-forming pancreatitis (n = 31)	Pancreatic carcinoma (n = 30)	X^2/t	P
Mass diameter (cm)	(3.56±2.05)	(3.04±1.46)	1.138	0.260
Sign of lobulation (%)	4 (12.90)	25 (83.33)	30.324	0.001
Mass calcification (%)	18 (58.06)	3 (10.00)	15.602	0.001
En plaque (n)	5	0		
Nodosity (n)	3	2		
Mixed type (n)	10	1		
Necrosis, cystic (%)	9 (29.03)	18 (60.00)	5.926	0.015
Pseudocyst (%)	18 (58.06)	3 (10.00)	15.602	0.001
Pancreatic duct stones (%)	15 (48.38)	5 (16.7)	16.120	0.014
Enhanced net increase CT value (HU)				
Arterial phase	24.45±9.80	13.90±5.45	5.172	0.001
Pancreatic parenchymal phase (portal venous phase)	45.40±14.55	35.80±10.10	2.984	0.004
High signal on DWI (%)	3 (9.68)	16 (53.33)	11.589	0.001
ADC value	1.35±0.12	1.00±0.10	12.350	0.001
Pancreatic duct dilation (%)	20 (64.52)	20 (66.67)	0.031	0.860
Uniform expansion (n)	3	18		
Beaded expansion (n)	17	2		
Pancreatic duct stones (%)	17 (54.84)	5 (16.67)	16.497	0.001
Bile duct dilation (%)	22 (70.97)	16 (53.33)	2.018	0.155
Right prerenal fascia thickening (%)	25 (80.65)	4 (13.33)	27.698	0.001
Peripancreatic vascular invasion (%)	22 (70.97)	24 (80)	0.531	0.562
Enlarged peripancreatic and retroperitoneal lymph nodes (%)	14 (45.16)	21 (70.00)	2.769	0.096

incidences of peripancreatic vascular invasion, lobulation signs, and necrotic cysts in the patients with pancreatic carcinoma were higher than they were in the patients with mass-forming pancreatitis. The incidences of calcification, pseudocysts, and pancreatic duct stones in the patients with pancreatic carcinoma were lower than they were in the patients with mass-forming pancreatitis ($P < 0.05$). In addition, the net enhanced CT value, the pancreatic parenchymal phase, and the pancreatic carcinoma ADC values were lower than they were in patients with mass-forming pancreatitis ($P < 0.05$). Finally, the rates of pancreatic duct stones and right prerenal fascia thickening in patients with pancreatic carcinoma were lower than they were in the patients with mass-forming pancreatitis ($P < 0.05$) (**Table 2**; **Figures 1**-**4**).

The diagnostic value of CT signs, MRI-DWI, MRCP and the combination of the three for pancreatic cancer

Based on the above results, peripancreatic vascular invasion, mass calcification, pseudocysts, pancreatic duct stones, the value of net enhanced CT in the arterial phase and the pancreatic parenchyma phase were selected as the CT signs of pancreatic masses, and the signs of lobulation, necrosis, high DWI signals, and low ADC values were selected as the main MRI-DWI, MRCP for pancreatic cancer. The results show that CT signs combined with MRI-DWI, MRCP can improve the diagnostic sensitivity for pancreatic cancer (**Table 3**).

The value of CT signs, MRI-DWI, MRCP, and their combined detection in the diagnosis of pancreatic cancer: The sensitivity and specificity of CT sign detection were 70.0% (21/30) and 70.0% (21/30), respectively. The sensitivity and specificity of MRI-DWI, MRCP were 78.5% (22/28) and 73.1% (22/30), respectively. The combined detection sensitivity of the two is 80% (24/30), and the specificity is 57.1% (24/42). The sensitivity of CT signs combined with MRI-DWI, MRCP was higher than it was for the single diagnosis (X2-14.778-MRI 0.000), thereby improving the clinical differential diagnostic ability (**Figure 5**).

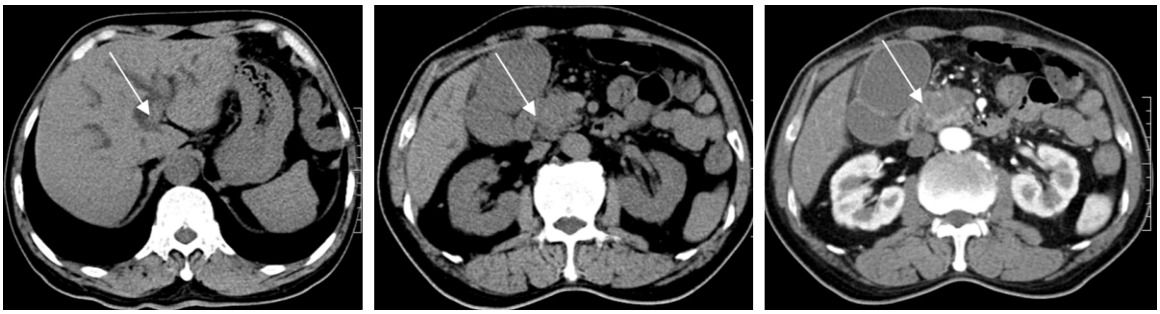

Figure 1. Enhanced CT of pancreatic cancer. The patient was diagnosed with pancreatic cancer. The pancreatic head was locally enlarged, the outline was irregular, and the density was uneven. The intrahepatic bile duct is dilated (black arrow). After the enhancement scanning, the pancreatic tissue was significantly enhanced in the arterial phase, but weak enhancement was seen in the location of the mass (white arrow). Note: CT: computed tomography.

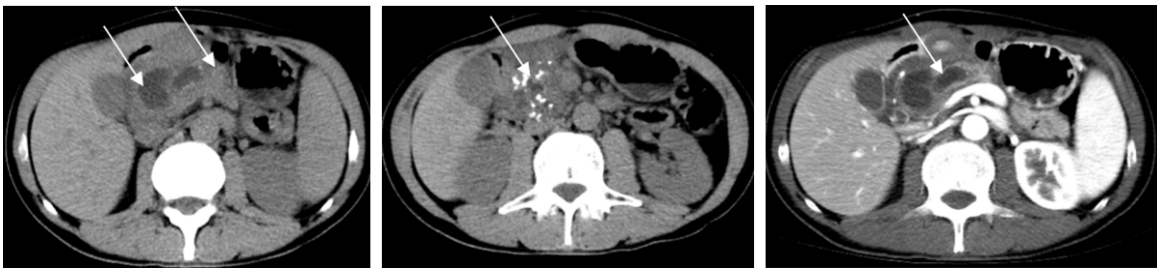

Figure 2. Enhanced CT of mass-forming pancreatitis. The patient was diagnosed with mass pancreatitis. The pancreatic head was enlarged and deformed, the edge of the pancreatic was unclear, and the cystic area (white arrow) and multiple nodular calcifications (white circle) could be seen in the mass area, along with an uneven enhancement of the mass in the arterial phase, and a significant dilatation of the main pancreatic duct (black arrow). Note: CT: computed tomography.

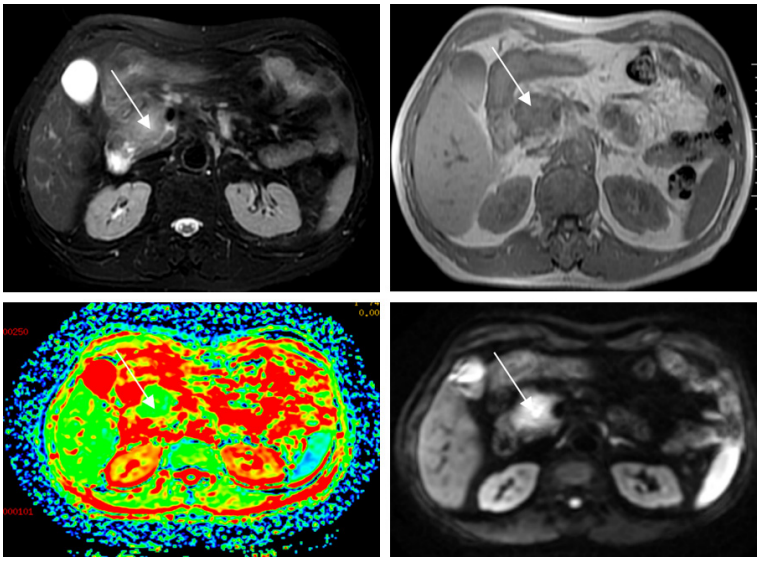

Figure 3. MRI-DWI of pancreatic cancer. The patient had a pancreatic carcinoma of the head of the pancreas, with uneven signal intensity and an unclear boundary. DWI showed high signals, and long T1 and T2 signal masses appeared with the head of the pancreas (white arrow). Note: MRI-DWI: magnetic resonance imaging with diffusion-weighted imaging.

Discussion

In our study, we found that peripancreatic vascular invasion, mass calcification, pseudocysts, pancreatic duct stones, and the values of net enhanced CT in arterial phase and pancreatic parenchyma phase were selected as the CT signs of pancreatic masses, and the signs of lobulation, necrosis, high DWI signals, and low ADC values were selected as the main MRI-DWI, MRCP for pancreatic cancer. Moreover, the study confirmed that the calcification and cystic signs of CT are the imaging manifestations of pancreatic masses. Necrosis, high DWI signals, and low ADC values are the diagnostic effects of

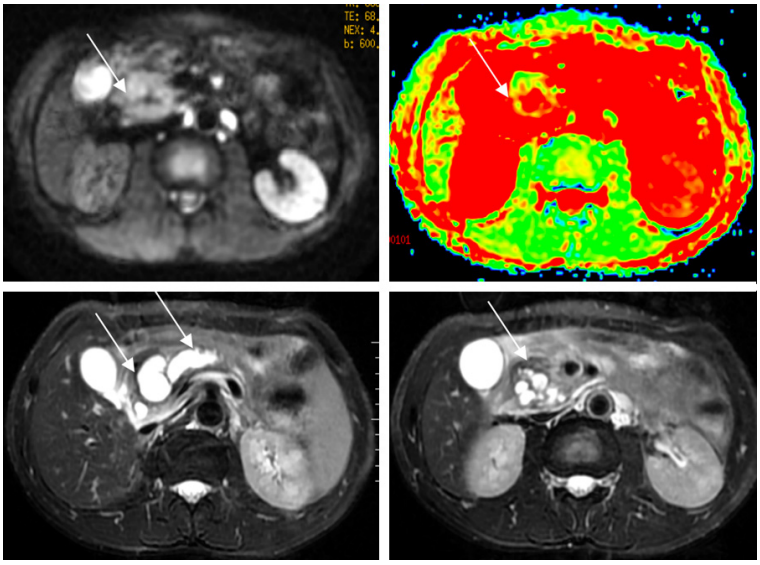

Figure 4. MRI-DWI of mass-forming pancreatitis. The patient was a mass type of pancreatitis with multiple cystic lesions (black arrow) in the head of the pancreas, dilatation of the main pancreatic duct (short white arrow) and slightly high signal on DWI (long white arrow). Note: MRI-DWI: magnetic resonance imaging with diffusion-weighted imaging.

Table 3. Comparison of the positive rate of clinical diagnosis with CT signs combined with 1.5T MRI-DWI, MRCP

Diagnostic index	CT sign		MRI-DWI, MRCP		CT sign with MRI-DWI, MRCP	
	+	-	+	-	+	-
Pancreatic mass group (n)	9	22	6	25	18	13
Pancreatic carcinoma group (n)	21	9	22	8	24	6

Note: CT: computed tomography; MRI-DWI: magnetic resonance imaging diffusion weighted imaging; MRCP: magnetic resonance cholangiopancreatography.

pancreatic cancer, and the diagnostic efficiency was analyzed. The results showed that CT signs combined with MRI-DWI. MRCP can improve the diagnostic sensitivity for pancreatic cancer.

Pancreatic carcinoma and mass-forming pancreatitis have poor specificities in the clinical features, the pathological basis between them is very similar, and the rate of misdiagnosis of benign masses is as high as 10%. The surgical exploration of pancreatic fibrous tissue hyperplasia and cancerous invasion caused by pancreatitis is more difficult [8, 9]. There was no significant difference in the clinical and biological indexes between carcinoma of the head of pancreas and mass-forming pancreatitis ($P > 0.05$). The main clinical manifestations of the patients include chronic abdominal pain accompanied by obstructive jaundice and a decreased body mass. Therefore, it is of great significance for patients to differentiate among pancreatic masses in the clinic [10, 11].

Previous studies have confirmed that mass-forming pancreatitis is characterized by diffuse calcification, a disturbance of the endocrine functions, which result in calcium salt deposition, pancreatic calcification, and pancreatic duct stone formation. On the other hand, most of the pancreatic cancer showed no calcification and less calcification, and it is often distributed in the necrotic area in the center of the mass. Therefore, preliminary differentiation can be achieved by an imaging observation of the calcification in the mass [12, 13]. The cystic change is also a common difference between the two imaging manifestations. Pancreatic carcinoma has more cysts and uneven wall thicknesses, uneven inner edges, and smooth inner edges of mass-forming pancreatitis. The pseudocyst of mass-forming pancreatitis is mainly distributed in the mass and the head of the pancreas, and it is often multiple in number and large in size. Currently, it has not been found in pancreatic cancer, but the number of cystic lesions in the mass and the imaging features can be used as the basis for a differential diagnosis of pancreatic cancer and mass-forming pancreatitis. This study also confirmed that calcification and cystic CT signs are also clinically sensitive, which is consistent with previous studies [14, 15].

Studies have shown that DWI has an important value in the diagnosis of cancer. DWI can effectively reflect the irregular thermal movement of water molecules in tissue, and it is closely related to the density of tissue cells [16, 17]. In the solid part of the tumor, the ADC value is increased along with the cell density and the

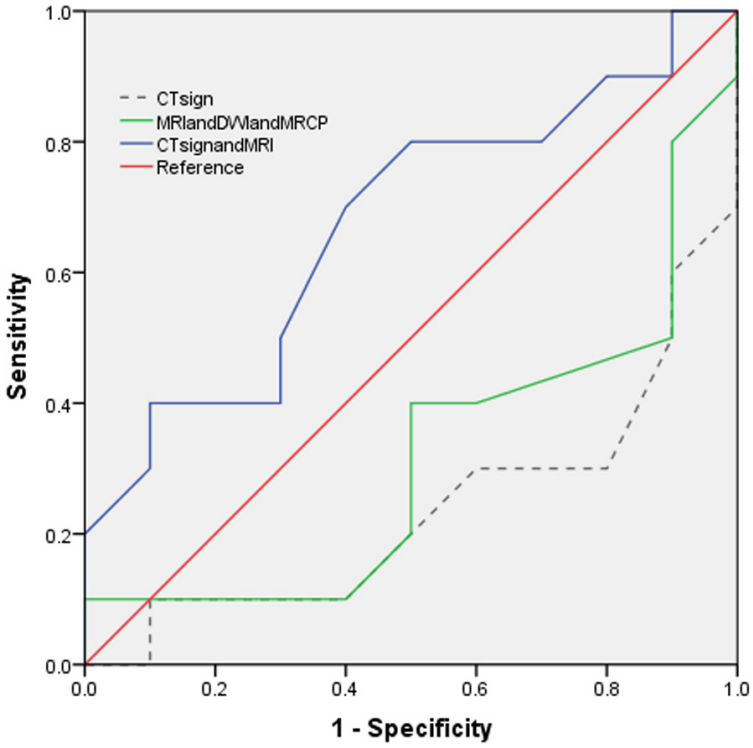

Figure 5. ROC curve of the diagnosis of pancreatic cancer.

diffusion disorders in the cell, so the activity of the water molecules in the cell is limited, and the ADC value decreased [18]. The signal intensity of pancreatic carcinoma lesions decreased in varying degrees, which lead to an increase in the contrast of lesions and pancreatic parenchyma and the significance of the manifestation of the pancreatic lesions. It plays an important auxiliary role in the qualitative diagnosis of the lesions. Therefore, the contrast between the high signal intensity of pancreatic carcinoma and the low signal intensity of mass-forming pancreatitis plays an important role in the differential diagnosis of pancreatic cancer and mass-forming pancreatitis [19]. Finally, necrosis is also an important manifestation. Our results demonstrated that along with the high ADC values, necrosis has a higher diagnostic sensitivity than CT, which supports the previous research [20]. Last but not least, the results of this study show that the combination of CT and MRI-DWI, MRCP can further improve the sensitivity of the clinical diagnosis of pancreatic carcinoma, which is higher than the single diagnostic method of pancreatic carcinoma.

However, there are several limitations to our research. The cohort of the patients with mass-forming pancreatitis or pancreatic carcinoma was small. On the other hand, our study didn't incorporate healthy people or any other kinds of pancreatic diseases to compare. Additionally, there exists a bias in this retrospective study because all the researchers knew that each subject had either mass-forming pancreatitis or pancreatic carcinoma. Therefore, further larger scale, randomized, controlled clinical trials may be needed to establish the usefulness of the evidence.

To sum up, CT signs combined with MRI-DWI, MRCP can improve the sensitivity of the clinical diagnosis of pancreatic carcinoma and the ability of the differential diagnosis of pancreatic carcinoma and mass-forming pancreatitis. However, there were differences in the imaging findings between the two kinds of pancreatic cancer and pancreatic masses in this study, such as the lobulation signs. In addition, the determination of the ADC values in this study is of great significance to further improving the clinical diagnostic value of the imaging.

Disclosure of conflict of interest

None.

Address correspondence to: Yongmei Li, Department of Radiology, The First Affiliated Hospital of Chongqing Medical University, No. 1 Youyi Road, Yuanjiagang, Yuzhong District, Chongqing 400016, China. Tel: +86-023-68899931; E-mail: lymzhang70@aliyun.com

References

[1] Bieliuniene E, Brøndum Frøkjær J, Pockevicius A, Kemesiene J, Lukosevičius S, Basevicius A, Atstupenaite V, Barauskas G, Ignatavicius P, Gulbinas A and Dambrauskas Z. CT- and MRI-based assessment of body composition and pancreatic fibrosis reveals high incidence of clinically significant metabolic changes that affect the quality of life and treatment outcomes

of patients with chronic pancreatitis and pancreatic cancer. Medicina (Kaunas) 2019; 55: 649.

[2] Hocker JR, Postier RG, Li M, Lerner MR, Lightfoot SA, Peyton MD, Deb SJ, Baker CM, Williams TL, Hanas RJ, Stowell DE, Lander TJ, Brackett DJ and Hanas JS. Discriminating patients with early-stage pancreatic cancer or chronic pancreatitis using serum electrospray mass profiling. Cancer Lett 2015; 359: 314-24.

[3] Bartell N, Bittner K, Vetter MS, Kothari T, Kaul V and Kothari S. Role of endoscopic ultrasound in detecting pancreatic cancer missed on cross-sectional imaging in patients presenting with pancreatitis: a retrospective review. Dig Dis Sci 2019; 64: 3623-3629.

[4] Bogveradze N, Hasse F, Mayer P, Rupp C, Tjaden C, Klauss M, Kauczor HU and Weber TF. Is MRCP necessary to diagnose pancreas divisum? BMC Med Imaging 2019; 19: 33.

[5] Goldfinger MH, Ridgway GR, Ferreira C, Langford CR, Cheng L, Kazimianec A, Borghetto A, Wright TG, Woodward G, Hassanali N, Nicholls RC, Simpson H, Waddell T, Vikal S, Mavar M, Rymell S, Wigley I, Jacobs J, Kelly M, Banerjee R and Brady JM. Quantitative MRCP imaging: accuracy, repeatability, reproducibility, and cohort-derived normative ranges. J Magn Reson Imaging 2020; 52: 807-820.

[6] Chou CT, Chen RC, Yang AD and Wu HK. Gallbladder torsion diagnosed by MDCT and MRCP. HPB 2018; S770.

[7] Pan ZW and Shen HL. Multispectral image super-resolution using structure-guided RGB image fusion. Pattern Recognition and Computer Vision 2018; 155-167.

[8] Honta S and Katanuma A. Diagnosis of resectable pancreatic cancer. Nihon Shokakibyo Gakkai Zasshi 2020; 117: 290-296

[9] Mayerle J, Kalthoff H, Reszka R, Kamlage B, Peter E, Schniewind B, González Maldonado S, Pilarsky C, Heidecke CD, Schatz P, Distler M, Scheiber JA, Mahajan UM, Weiss FU, Grützmann R and Lerch MM. Metabolic biomarker signature to differentiate pancreatic ductal adenocarcinoma from chronic pancreatitis. Gut 2018; 67: 128-137.

[10] Puleo F, Maréchal R, Demetter P, Bali MA, Calomme A, Closset J, Bachet JB, Deviere J and Van Laethem JL. New challenges in perioperative management of pancreatic cancer. World J Gastroenterol 2015; 21: 2281-93.

[11] Dite P, Novotny I, Dvorackova J, Kianicka B, Blaho M, Svoboda P, Uvirova M, Rohan T, Maskova H and Kunovsky L. Pancreatic solid focal lesions: differential diagnosis between autoimmune pancreatitis and pancreatic cancer. Digestive diseases (Basel, Switzerland) 2019; 37: 1-6.

[12] Sedhai YR and Patel D. Calcific pancreatitis associated with alcohol use. N Engl J Med 2017; 376: e6.

[13] Rana SS, Sharma R and Gupta R. Pancreatic parenchymal calcification induced by permanent indwelling transmural stent. JGH Open 2019; 3: 264-265

[14] Almeida RR, Lo GC, Patino M, Bizzo B, Canellas R and Sahani DV. Advances in pancreatic CT imaging. AJR Am J Roentgenol 2018; 211: 52-66.

[15] Sandrasegaran K, Lin Y, Asare-Sawiri M, Taiyini T and Tann M. CT texture analysis of pancreatic cancer. Eur Radiol 2019; 29: 1067-1073.

[16] Wu L, Li J, Fu C, Kühn B and Wang X. Chemotherapy response of pancreatic cancer by diffusion-weighted imaging (DWI) and intravoxel incoherent motion DWI (IVIM-DWI) in an orthotopic mouse model (Article). MAGMA 2019; 32: 501-509.

[17] Li J, Liang L, Yu H, Shen Y, Hu Y, Hu D, Tang H and Li Z. Whole-tumor histogram analysis of non-Gaussian distribution DWI parameters to differentiation of pancreatic neuroendocrine tumors from pancreatic ductal adenocarcinomas. Magn Reson Imaging 2019; 55: 52-59.

[18] Dalah E, Erickson B, Oshima K, Schott D, Hall WA, Paulson E, Tai A, Knechtges P and Li XA. Correlation of ADC with pathological treatment response for radiation therapy of pancreatic cancer. Transl Oncol 2018; 11: 391-398.

[19] Wolske KM, Ponnatapura J, Kolokythas O, Burke LMB, Tappouni R and Lalwani N. Chronic pancreatitis or pancreatic tumor? A problem-solving approach. Radiographics 2019; 39: 1965-1982.

[20] Mohamed E, Sanghera B and Wong W. Does tumour SUVmax predict adverse prognostic features in patients with pancreatic cancer? HPB 2018; 20: S771.